PCCP

PAPER

View Article Online
View Journal | View Issue

Cite this: *Phys. Chem. Chem. Phys.*, 2021, **23**, 20340

Prediction of the standard potentials for one-electron oxidation of *N,N,N′,N′* tetrasubstituted *p*-phenylenediamines by calculation†

Cecilie L. Andersen, [a] Evanildo G. Lacerda Jr, [b] Jørn B. Christensen, [c] Stephan P. A. Sauer *[a] and Ole Hammerich *[a]

Received 25th May 2021,
Accepted 31st August 2021

DOI: 10.1039/d1cp02315b

rsc.li/pccp

The formal potentials for the reversible one-electron oxidation of *N,N,N′,N′* tetrasubstituted *p*-phenylenediamines in acetonitrile have been applied as a test set for benchmarking computational methods for a series of compounds with only small structural differences. The aim of the study is to propose a simple method for calculating the standard oxidation potentials, and therefore, the protocol is progressively developed by adding more terms in the energy expression. In addition, the effect of including implicit solvation models (IEFPCM, CPCM, and SMD), larger basis sets, and correlation methods are investigated. The oxidation potentials calculated using the G3MP2B3 approach with IEFPCM resulted in the best fit (R^2 = 0.9624), but the slope of the correlation line, 0.74, is far from the optimal value, 1.00. B3LYP/6-311++G(d,p) and TPSSh/6-311++G(2d,p) yielded only slightly less consistent data (R^2 = 0.9388 and R^2 = 0.9425), but with much better slopes, 1.00 and 0.94, respectively. We conclude that it is important to investigate the basis set size and treatment of electron correlation when calculating oxidation potentials for *N,N,N′,N′* tetrasubstituted *p*-phenylenediamines.

Introduction

Standard potentials, E°, or more broadly speaking redox potentials, are fundamental properties in the characterization of chemical reduction and oxidation reactions. Examples from organic chemistry and biochemistry include not only molecular electrochemistry,[1,2] but also electron–reservoir complexes,[3] syntheses with regenerable redox systems,[4] photoredox catalysis,[5] proton coupled electron transfer,[6,7] electronics[8] and electrochromic materials,[9] materials for solar cells,[10,11] molecular conductors[12] and conducting polymers,[13] redox proteins,[14–16] artificial photosynthesis,[17–19] reduction of carbon dioxide[20] and many, many more.

Among the redox reactions, simple one-electron transfers have received special attention.[1,2,21–27] Experimentally, standard potentials for one-electron transfers are typically determined by electrochemical methods such as cyclic voltammetry (CV) and differential pulse voltammetry (DPV) although, strictly speaking, the potentials determined by CV and DPV are formal potentials, $E^{\circ\prime}$, and not standard potentials, E°.[2,28] However, the difference is only small for most organic compounds and may be neglected for practical purposes. The initial products resulting from one-electron transfer to or from closed-shell molecules, the radical anions and radical cations, are usually reactive species[1,2,29–33] and only in few cases persistent under the conditions of routine CV and DPV. This is true in particular in aqueous solution because of the electrophilic and nucleophilic properties of water. Persistent radical ions in nominally dry non-aqueous solutions include the radical anions and radical cations of alternant aromatic hydrocarbons, the radical anions of compounds containing electron-withdrawing groups such as nitro, cyano and carbonyl and the radical cations of heteroaromatic compounds containing O, S or N or compounds containing electron-donating substituents such as dialkylamino and alkoxy.[1,2] In most other cases, the formal potentials can only be determined experimentally with difficulty, if at all. In such cases quantum chemical calculations provide an important alternative to experiments, for example for the prediction of the redox potentials for free radicals[34–36] and carbenes[37] and for substrates that undergo dissociative electron transfer.[38,39]

Early it was found that the coefficients of the molecular orbital resonance integral in the Hückel expression for the energy of the lowest unoccupied molecular orbital (LUMO)

[a] *Department of Chemistry, University of Copenhagen, Universitetsparken 5, DK-2100 Copenhagen Ø, Denmark. E-mail: sauer@kiku.dk, o.hammerich@chem.ku.dk*
[b] *Instituto de Física da Universidade de São Paulo, Rua do Matão 1371, 05508-090 São Paulo, SP, Brazil*
[c] *Department of Chemistry, University of Copenhagen, Thorvaldsensvej 40, DK-1871 Frederiksberg C, Denmark*

† Electronic supplementary information (ESI) available: Chemicals, electrochemistry – CV and DPV curves, and computational output. See DOI: 10.1039/d1cp02315b

were linearly related to the reduction potentials of a series of conjugated hydrocarbons.[40] This inspired a number of similar investigations including the linear relation between the energies of the highest occupied molecular orbital (HOMO) and the oxidation potentials for conjugated hydrocarbons.[41–49] These early efforts have been briefly reviewed.[50] Shortly after self-consistent field (SCF) improvements were reported[51,52] and in the years to follow, such correlations were extended to include computed values of the HOMO and LUMO energies, E_{HOMO} and E_{LUMO}, and of the ionization potentials (IP) and electron affinities (EA).[53–65] Once established such linear relations are useful, but still the ultimate goal is the direct calculation of the redox potentials.

Two different approaches have been followed for the calculations. One is based on a Born–Haber cycle in which the solution free energy difference between the reduced and oxidized forms are obtained from the gas phase values by addition of the free energies of solvation for the two oxidation states. The other is more direct and uses the solution free energies computed with the application of a suitable solvation model. Often, the free energies are obtained by density functional theory (DFT) calculations using the B3LYP functional and a Pople-type basis set as illustrated by, for instance, the reduction of polycyclic aromatic hydrocarbons (PAH)[66] and quinones,[67–69] the oxidation of PAH[66] and alkylbenzenes[60] and recipes for organic molecules in general.[70–75] Other DFT functionals such as BPW91 for the oxidation of substituted anilines.,[76] mPWB1K[77] and PBE[78] for the reduction of aromatic nitro compounds and M06-2X and CAM-B3LYP for the redox potentials azulene-1-carbonitriles[79] have been advocated as well and occasionally also HF, for example, for the reduction of quinones[61,80] and various CBS variants.[58] Common to all these approaches is the need for an adequate solvation model,[81] as for example the PCM,[82–84] the CPCM,[85,86] the SMD[87] and the SM5.42R.[88] Useful overviews describing these various approaches are available.[89,90]

Looking back on all this, there is a shortage of studies dedicated to the prediction of the redox potentials for a series of closely related substrates such as π-systems perturbated by substituents that exert their influence only by classical inductive effects. In fact, we are aware of only one such study, that is the calculation of the oxidation potentials of a series of alkylbenzenes[60] for which the experimental data had been published earlier.[91] One reason for the shortage of such studies is without doubt that the compounds of interest are not readily available and have to be synthesized.

We have for some time been engaged in using *N*,*N*,*N*′,*N*′ tetrasubstituted *p*-phenylenediamines as redox catalysts[92–94] and as cores in redox active dendrimers[95,96] and were for that reason interested in the prediction of the oxidation potentials by calculation.

N,*N*,*N*′,*N*′ tetrasubstituted *p*-phenylenediamines

N,*N*,*N*′,*N*′ tetrasubstituted *p*-phenylenediamines are electron-rich compounds that are easily oxidized to persistent radical cations by, for instance, electrochemical oxidation.[94–102] A famous member of the group is *N*,*N*,*N*′,*N*′-tetramethyl-*p*-phenylenediamine (TMePD) the radical cation of which (Wurster's blue) was reported as early as 1879.[103] Since then the radical cations of TMePD and related *p*-phenylenediamines have featured in numerous investigations including studies of the optical,[104] vibrational[105,106] and ESR spectra,[107–112] electronic,[113–116] mixed-valence[117,118] and self-exchange properties,[119–122] reorganization energies,[123] and radical cation dimerizations.[124–126] Also, TMePD has been used in electron transfer studies,[127,128] and in charge-transfer complexes,[129–131] as a redox mediator,[132–134] and in studies of solvent effects on redox properties.[135,136] In spite of this overwhelming and continuing interest, the effect of the nature of the N-substituent on the oxidation potential have not been thoroughly investigated and the possibility of predicting the oxidation potentials of new derivatives by calculation has not been addressed in any detail.

Here we present experimental and computed potentials for the one-electron oxidation of a series of *N*,*N*,*N*′,*N*′ tetrasubstituted *p*-phenylenediamines. We will examine computational protocols for the oxidation potentials at several levels of complexity, from the simple HOMO approximation to the full Gibbs free energy description. The influence of the solvation models, basis set size and correlation methods will be investigated as well.

The structures of the sixteen *N*,*N*,*N*′,*N*′-tetrasubstituted *p*-phenylenediamines included in this study are shown in Fig. 1 and Table 1.

Experimental and computational methods

Syntheses. Only one compound, TMePD, is commercially available (Aldrich). The other 15 were prepared as described in the ESI.†

Cyclic voltammetry and differential pulse voltammetry. CV and DPV measurements were carried out at room temperature using an Autolab PGSTAT12 instrument driven by the GPES 4.9 software. The solvent was acetonitrile (MeCN) containing Bu_4NPF_6 (0.1 M) as supporting electrolyte. The working electrode was a circular glassy carbon disk (d = 3 mm), the counter electrode was a platinum wire and the reference electrode was a silver wire immersed in the solvent–supporting electrolyte mixture and physically separated from the solution containing the substrate by a ceramic frit. The potential of the reference electrode was determined *vs.* the ferrocene/ferrocenium (Fc/Fc^+) redox couple[137] in separate experiments. The concentration of substrate was 1 mM. Solutions were purged with argon saturated with MeCN for at least 10 minutes before the measurements were made after which a stream of argon was

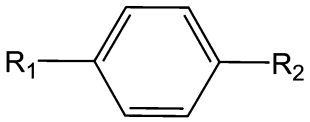

Fig. 1 General structure of the *N*,*N*,*N*′,*N*′ tetrasubstituted *p*-phenylenediamines. The substituents, R_1 and R_2, that include the two N-atoms, are shown in Table 1.

Table 1 The abbreviations used, the substituents, R_1 and R_2, in Fig. 1 and the formal potentials, $E^{\circ\prime}_{exp}$, for one-electron oxidation[a]

Compound	$E^{\circ\prime}_{exp}$	R_1	R_2	Compound	$E^{\circ\prime}_{exp}$	R_1	R_2
TMePD	−0.282			DMeAzirA	+0.089		
TrMeEtPD	−0.302			DMeAzetA	−0.290		
DMeDEtPD	−0.321			DMeMorphA	−0.161		
TEtPD	−0.361			DMePiprzA	−0.221		
TrMeiPrPD	−0.301			DMeMePiprzA	−0.197		
DMeDiPrPD	−0.317			BPyrB	−0.397		
TiPrPD	−0.297			BPipB	−0.216		
DHDiPrPD	−0.283			BMorphB	−0.053		

[a] Recorded by DPV in MeCN (0.1 M Bu_4PF_6) and given in V *vs.* Fc/Fc^+.

maintained over the solutions. The CV voltage scan rate was 0.1 V s^{-1}. The DPV parameters were the following: step potential 2 mV; modulation amplitude 25 mV; modulation time 50 ms; interval time 0.5 s; scan rate 4 mV s^{-1}. iR-Compensation was applied when adequate.

Computational strategy. *N*,*N*,*N*′,*N*′ tetrasubstituted *p*-phenylenediamines exist in many conformations, the number depending on the structure of the substituents. Test computations showed that the conformer of lowest free energy depended not only on the geometry around the two pyramidal or nearly pyramidal nitrogen atoms, but also, for example, on the orientation of the N–H hydrogen atom in DMePiprzA and the N–Me methyl group in DMeMePiprzA. Also, we found that the lowest free energy conformers were not the same for all solvation models. As a result of this, it was decided to investigate all conformers for all computational strategies. The output files for the neutrals and radical cations that we found to be of lowest free energy in the gas phase (B3LYP/6-31G(d,p)) are summarized in the ESI.†

A variety of progressively improved models were examined for the prediction of the oxidation potentials. As a starting point, E_{HOMO} for the neutral molecules were calculated and improvements were subsequently obtained (1) by calculation of the electronic energy differences, ΔE^*_{elec}, between the neutral and the radical cation using the optimized geometry for the neutral molecule, (2) by allowing geometry relaxation for the radical cation in the previous calculation, ΔE_{elec}, (3) by inclusion of the zero-point vibrational corrections to obtain the adiabatic ionization potential, IP_a, (4) by inclusion of the thermal and entropic corrections to obtain the gas phase Gibbs free energy difference, E^0_{calc}, where −0.03766 V was used for the energy of the free electron,[138] and finally (5) we examined the solvent and basis set size effects and the effect of different methods to treat the electron correlation.

All calculations for models (1)–(4) were carried out at the level of density functional theory using the B3LYP exchange–correlation functional.[139] In step (5) solvent effects were included by using the implicit solvent models IEFPCM,[83,84] CPCM,[85,86] and SMD[87] using the default values for the atomic radii and the electrostatic scaling factor. The influence of increasing the basis set was tested using various Pople,[140–143] Dunning,[144,145] and Jensen[146,147] basis sets. Further attempts to improve the description were made by using the range-separated hybrid functional ωB97XD with Grimme's D2 dispersion correction,[148] the meta-hybrid GGA functional TPSSh,[149,150] the second order Møller–Plesset perturbation theory (MP2),[151,152] and finally also the G3MP2B3 scheme.[153] Calculations at the MP2 and G3MP2B3 levels might still be too time consuming for routine applications and are included here only for comparison. The possible effect of dispersion was further investigated by adding Grimme's D3 empirical dispersion correction with the Becke–Johnson damping, GD3BJ, to the B3LYP functional.[154]

All calculations were carried out with the Gaussian 09 suite of programs.[155]

Results and discussion

Electrochemistry

The formal potentials for the one-electron oxidation of a number of *N*,*N*,*N*′,*N*′ tetrasubstituted *p*-phenylenediamines are available in the literature.[94–102] However, the experimental conditions are not always the same and in order to have a consistent data set for all compounds it was decided to

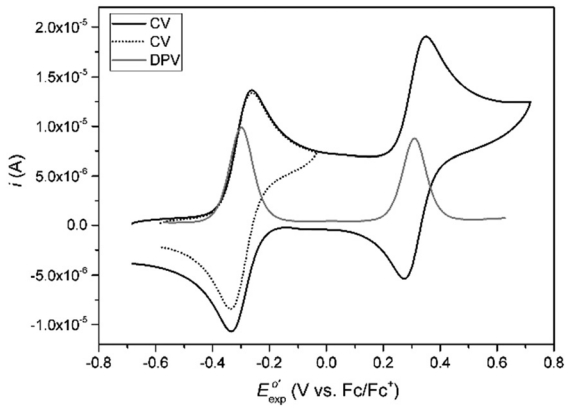

Fig. 2 Voltammograms of TrMeiPrPD (1 mM) recorded by CV and DPV in MeCN (0.1 M Bu_4NPF_6).

determine the formal potentials for all compounds as a part of this study.

A typical voltammogram is shown in Fig. 2 that includes also the corresponding DPV curve. (A complete set of CV and DPV curves is found in the ESI†). It is seen that the oxidation of the *N*,*N*,*N*′,*N*′ tetrasubstituted *p*-phenylenediamines to the radical cations proceeds reversibly and for most of the compounds, also the second electron transfer leading to the dication was observed. The formal potentials, $E^{\circ\prime}_{exp}$, recorded by DPV are summarized in Table 1.

The oxidation of the simple alkyl derivatives spans a potential range of only 79 mV (from −0.282 to −0.361 V for TMePD and TEtPD, respectively). In contrast, the potentials for compounds containing one or two heterocyclic rings span a much larger range of 486 mV (from −0.397 to +0.089 V for BPyrB and DMeAzirA, respectively) encompassing the range spanned by the alkyl-substituted derivatives. The compound most difficult to oxidize is DMeAzirA at +0.089 V for which the aziridine substituent introduces large geometric strain. On the other hand, the almost planar neutral BPyrB with two pyrrolidine units is most easily oxidized at −0.397 V. It is seen also the compound containing a five-membered ring system, BPyrB, is no less than 181 mV easier to oxidize than the six-membered analogue, BPipB. This rather big difference has been proposed to reflect the difficulty in attaining a planar geometry around the N-atom in the radical cation of the six-membered piperidine derivative.[99,100] Finally, comparison of the data for the series of compounds having a conformationally restricted six-membered ring substituents, which are all more difficult to oxidize than even TMePD, demonstrates a considerable effect of substitution in the remote C-2 position. The difference between the extreme values obtained for BPipB and BMorphB amounts to no less than 163 mV. This strong dependence of the formal potentials on the nature of the substituents is in agreement with the observations made by others.[94,98–100]

Computational chemistry

In the following, we will discuss the performance of each of the computational models individually. The approach is hereby always to plot the experimental formal potentials, $E^{\circ\prime}_{exp}$, against the calculated energies and to analyse the correlation by the least squares linear regression method. The results are summarized in Table 2 and, later, in Table 3. The quality of the correlations is evaluated by the goodness of the fit as expressed through the coefficient of determination, R^2, and by the slope and intercept of the correlation line. In the ideal case where the calculations mimic the experiment this would lead to an R^2 value and a slope of 1.000 and an intercept equal to the absolute potential of the Fc/Fc$^+$ redox couple. However, the latter is not a measureable quantity and therefore a lot of effort has been put into determining the value in other ways.[66,156,157] For example, the absolute potential of the Fc/Fc$^+$ half reaction was calculated to be −4.99 V at the G3(MP2)-RAD-Full-TZ level of theory using the COSMO-RS solvation model,[157] while a combined experimental and theoretical approach predicted a value of −5.22 ± 0.11 V.[66] Since the value is not known accurately, the calculated potentials of the *N*,*N*,*N*′,*N*′ tetrasubstituted *p*-phenylenediamines will in the following be benchmarked against the values resulting from both these studies.

Table 2 The intercept, slope and values of R^2 obtained from linear regression least squares method for several theoretical strategies all at the B3LYP/6-31G(d,p) level

Computed parameter	Solvation model	Slope	Intercept (V)	R^2
E_{HOMO}	None	0.29	−1.55	0.8172
ΔE^*_{elec}	None	0.30	−2.06	0.8383
ΔE_{elec}	None	0.67	−4.00	0.8798
IP_a	None	0.72	−4.33	0.8995
E°_{calc}	none	0.85	−5.00	0.8878
	IEFPCM	1.09	−4.77	0.9603
	CPCM	1.07	−4.66	0.9411
	SMD	1.02	−4.23	0.9802

Table 3 The intercept, slope, and values of R^2 obtained by linear least squares regression for the E°_{calc} calculated by several computational methods including the IEFPCM solvation model

Method	N^a	Slope	Intercept (V)	R^2
B3LYP/6-31G(d,p)	16	1.09	−4.77	0.9603
B3LYP/6-311++G(d,p)	16	1.00	−4.66	0.9388
B3LYP-GD3BJ/6-311++G(d,p)	16	0.98	−4.54	0.9052
ωB97XD/6-311++G(d,p)	16	0.91	−4.34	0.9120
TPSSh/6-311++G(2d,p)	16	0.94	−4.22	0.9425
MP2/6-31G(d,p)	15[b]	0.66	−3.12	0.9589
G3MP2B3	16	0.74	−3.72	0.9624

[a] *N* = number of data points. [b] DHDiPrPD was excluded from the fit.

***E*$_{HOMO}$.** Even though Koopmans' theorem does not apply to the DFT calculated HOMO energies, the values of E_{HOMO} are often used in correlations with $E^{\circ\prime}_{exp}$ as pointed out in the introduction. For this reason, the E_{HOMO} energies were included in the present study.

The correlation between E_{HOMO} and $E^{\circ\prime}_{exp}$ results in a rather low value of R^2 (0.8172) (Table 2 and Fig. 3), despite the fact that the largest outlier, DMeAzirA, represented by a ★ in Fig. 3, was not included in the least square fitting. DMeAzirA is the only compound with a positive formal potential and has the

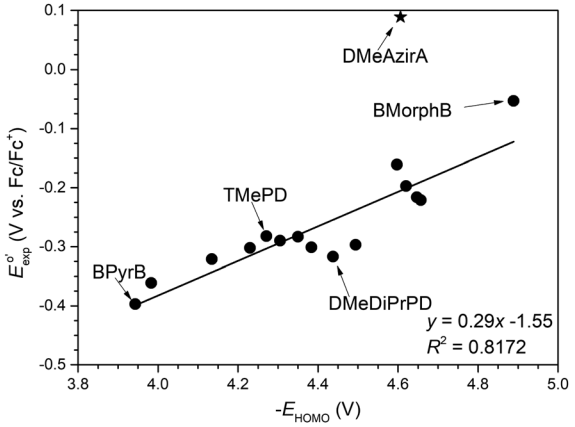

Fig. 3 Plot of $E^{\circ\prime}_{\mathrm{exp}}$ *vs.* E_{HOMO} calculated at the B3LYP/6-31G(d,p) level of theory. The data point represented by a star (★) is that for DMeAzirA (see the text) and is not included in the linear regression.

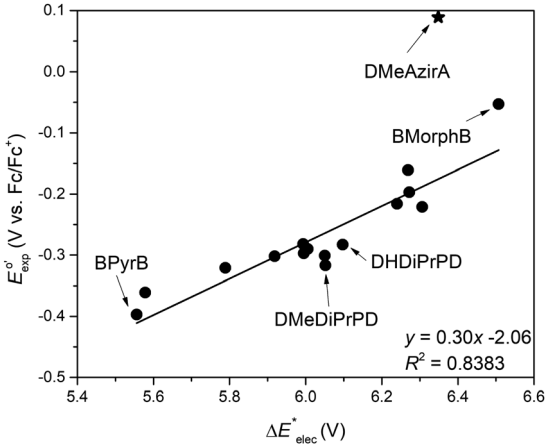

Fig. 4 Plot of the experimental $E^{\circ\prime}_{\mathrm{exp}}$ *vs.* the computed E^{*}_{elec} calculated at the B3LYP/6-31G(d,p) level of theory. The data point represented by a star (★) is for DMeAzirA and is not included in the linear regression.

highly strained three membered aziridine ring as one of the substituents. In addition, two minor outliers, BMorphB and DMeDiPrPD, were observed. Not unexpectedly, the slope and intercept, 0.29 and −1.55 V, are not even close to the optimal values.

A problematic issue regarding this model is the question of how to choose the most stable conformer. Most consistent with the idea of a cheap and quick estimation of the potentials using this model would have been to choose the lowest energy conformer based on the electronic energy. On the other hand, in order to check whether the found conformer is actually a local minimum, one anyway has to calculate the frequencies and thus obtains the Gibbs free energy. Therefore, we have also for this model chosen to base our selection of the conformers on the Gibbs free energy. This leads then in several cases to different conformers as one would choose based on the electronic energies. An example is TMePD, where the *syn*-conformer has the lower electronic energy, but the *anti*-conformer the lower Gibbs free energy. For E_{HOMO} this leads, however, only to a change of 0.1%. One of the larger outliers is DMeDiPrPD, for which there are many different orientations of the substituents at the two N-atoms. In this case E_{HOMO} of the three conformers with the lowest Gibbs free energy differ by only 0.5% at most. Although the effect is not big, it is indeed noticeable.

Electronic energies. Electronic relaxation is introduced by calculating the potential energy as the difference between the total electronic energies of both species, $\Delta E^{*}_{\mathrm{elec}}$ (see Fig. 4). In this model, however, the geometry of the neutral molecule is used for both species. The value of R^2, still without DMeAzirA, now equals 0.8383, which is a rather small increase by only 3% compared to the E_{HOMO} correlation (Table 2). Furthermore, the slope of the correlation only improves marginally to 0.30, while the intercept is somewhat improved to −2.06 V. Nevertheless, the correlation is very similar as that for E_{HOMO}. Also, the outliers from the correlation line are still the same, DMeAzirA, which was not included in the linear regression, and BMorphB and DMeDiPrPD. All this despite the fact, that the electronic energies are roughly 1.6 V higher than E_{HOMO} as judged by BPyrB at the lower and BMorphB at the higher end.

The correlation is slightly improved by 5%, resulting in a value of R^2 = 0.8798 when also the geometry of the radical cation is relaxed, ΔE_{elec} (Table 2 and Fig. 5). However, this comparison is not quite fair as the point for DMeAzirA is now included in the correlation. More important, both the slope 0.67 and the intercept −4.00 V are much improved in this model due to the relaxation of the geometry of the radical cations. On average their electronic energies are reduced by 0.45 V. But more important for the improvement of the slope and intercept is that the relaxation effect is larger than the average for the compounds, which had the larger values of $\Delta E^{*}_{\mathrm{elec}}$ such as DMePiprzA, DMeMePiprzA, BPipB, BMorphB, TiPrPD and DMeDiPrPD, whereas the molecules with the smallest $\Delta E^{*}_{\mathrm{elec}}$ values also exhibit the smallest relaxation effects: BPyrB, TEtPD and DMeDEtPD. All together, the correlation is much better than the one for E_{HOMO} and $\Delta E^{*}_{\mathrm{elec}}$. DMeAzirA, which used to be the largest outlier, is still a bit

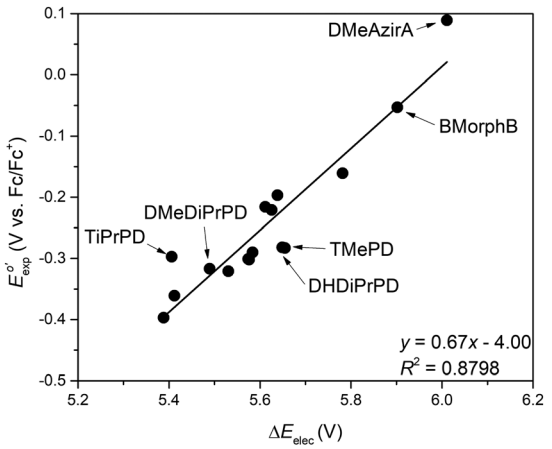

Fig. 5 Plot of the experimental $E^{\circ\prime}_{\mathrm{exp}}$ *vs.* the computed ΔE_{elec} calculated at the B3LYP/6-31G(d,p) level of theory.

off, but its data point is now much more consistent with the other points. However, this is not due to a particular large relaxation effect for DMeAzirA, which with 0.34 V is smaller than the average. The reason is the before mentioned large relaxation effects for the other compounds. Also in the case of the other outliers in Fig. 4, BMorphB and DMeDiPrPD, geometry relaxation of the radical cation brought them in perfect agreement with the linear regression curve. On the other hand, TiPrPD and TMePD, which have very similar formal potentials, $E^{\circ\prime}_{\mathrm{exp}}$, and also had similar values of $\Delta E^{*}_{\mathrm{elec}}$ have quite different values of ΔE_{elec} due to a significantly smaller relaxation effect for TMePD. They are both outliers now in Fig. 5 together with DHDiPrPD, which already was an outlier in Fig. 4.

The overall large effect of the geometry relaxation of the radical cations on their energy was expected. It is due to the large structural reorganization accompanying the oxidation. Primarily this involves that the preferred geometry around the N-atom in the radical cations is planar, whenever this is possible. Based on these calculations the electronic and geometric relaxation are not unexpectedly concluded to be important contributions to the energy expression for calculating oxidation potentials.

IP_a. A refinement of representing the oxidation potentials by ΔE_{elec}, *i.e.* the difference in electronic energy between the two minima, is achieved by including the zero-point vibrational correction terms, ΔE_{ZPVC}, to the total electronic energy difference, ΔE_{elec}. This is the adiabatic ionization potential, IP_a. Compared to the results obtained as ΔE_{elec}, the IP_a method slightly improves the value of R^2 (0.8995) with 2% (Table 2 and Fig. 6) and further improves the slope to now 0.72 and the intercept to −4.33 V. However, Fig. 6 shows still the same outliers DMeAzirA, TiPrPD, TMePD and DHDiPrPD as without inclusion of the zero-point vibrational corrections. Nevertheless, we conclude that the vibrational correction term does have a positive impact on the correlation.

Gibbs free energy difference (gas phase). Finally, in the following models the proper thermodynamic quantity for the calculation of oxidation potentials is used, *i.e.* the difference in Gibbs free energies. Therefore, we will now use the symbol, $\Delta E^{\circ}_{\mathrm{calc}}$. This implies that we augment IP_a with the differences in entropy and in the thermal contributions to the enthalpy and subtract a small correction term, 0.03766 V, which corresponds to the energy of the free electron at 298 K.[138]

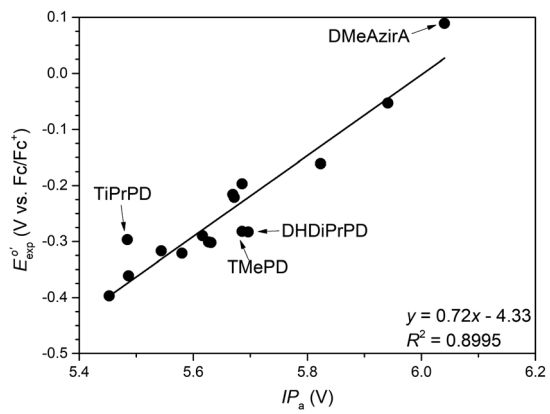

Fig. 6 Plot of the experimental $E^{\circ\prime}_{\mathrm{exp}}$ *vs.* the computed IP_a calculated at the B3LYP/6-31G(d,p) level of theory.

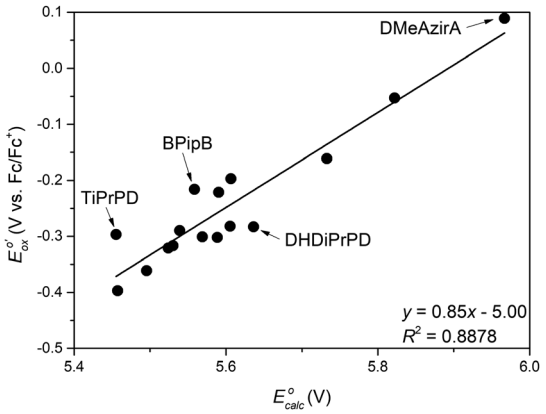

Fig. 7 Plot of the experimental $E^{\circ\prime}_{\mathrm{exp}}$ *vs.* $E^{\circ}_{\mathrm{calc}}$ calculated at the B3LYP/6-31G(d,p) level of theory.

Calculating the potentials as $\Delta E^{\circ}_{\mathrm{calc}}$ further improves the slope (0.85) and intercept (−5.00 V) compared to the results obtained at the IP_a level (Table 2 and Fig. 7), while the value of R^2 (0.8878) is slightly worse than for the IP_a level. DMeAzirA is now no longer an outlier in relation to the linear regression line, while TiPrPD and DHDiPrPD still are. In addition, the calculated potential for BPipB is also somewhat too small.

A decomposition of the percentage contribution of each term in ΔG shows that on average the ΔE_{elec} contribution accounts for 99.6%, the ΔE_{ZPVC} for 0.9%, the $\Delta E_{\mathrm{thermal}}$ for 0.1% and the entropic term $T\Delta S$ for 0.5%. Therefore, the electronic energy accounts for almost all the energy involved in the Gibbs free energy difference for these molecules, and accurate calculations of it should be the focus in order to improve the models.

Gibbs free energy difference (solution). In order to describe the influence of the environment of the solute during the experiment, implicit solvation models were included in the next step of our computational strategy. In the implicit solvation models, the solvent properties are represented by the dielectric constant (MeCN: 35.7),[158] but one should keep in mind that the experimentally determined potentials were obtained in a mixture of MeCN and supporting electrolyte, resulting in an increased dielectric constant for solvents with low and medium permittivity.[159] Furthermore, the implicit continuum models also neglect specific solute–solvent interactions, which were found to have some effect on, *e.g.*, the proton NMR chemical shifts of N–H in protonated pyrroles.[160,161]

The $E^{\circ}_{\mathrm{calc}}$ energies calculated with and without implicit solvation models are presented in Fig. 8. In this and the following figures the results are compared with the optimal correlations with the function $y = 1x - 5.22$ (solid red) and $y = 1x - 4.99$ (dashed red) using the two different suggested

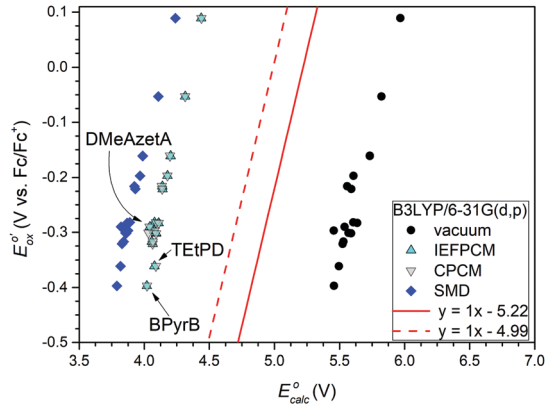

Fig. 8 Plot of the experimental $E^{o'}_{exp}$ *vs.* ΔE^{o}_{calc} using implicit solvation models. The ideal correlations with intercept −5.22 V (---) and −4.99 V (- -) are shown.

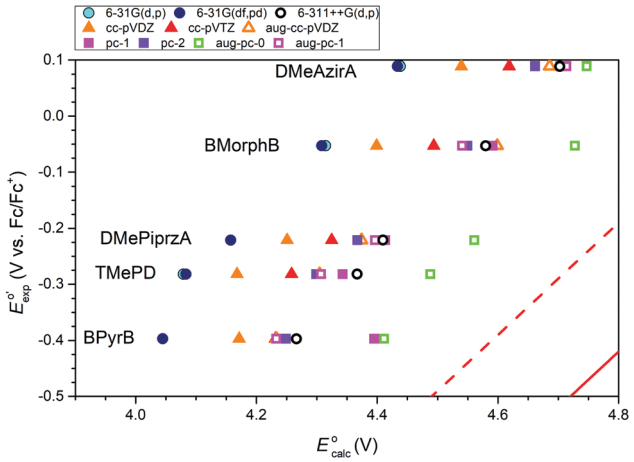

Fig. 9 Selection of basis sets tested in the basis set analysis for the B3LYP functional including the implicit solvation model IEFPCM. The ideal correlations with intercept −5.22 V (---) and −4.99 V (- -) are shown.

potentials for the Fc/Fc$^+$ redox couple.[66,157] The results of the linear regression for the three solvent models are given in Table 2. The calculated potentials decrease when implicit solvation models are included as compared to the results obtained without solvation (the data sets are moved to the left); a phenomenon most pronounced for the results obtained using the SMD model, which differs from the IEFPCM by employing different radii and non-electrostatic terms.[87] The data obtained by the IEFPCM and CPCM models are very similar (cannot be distinguished in Fig. 8). A comparison of the correlation equations obtained with and without implicit solvation models (in Table 2) reveals that the implicit solvation models on one hand significantly improve the slope to between 1.02 and 1.09 compared to 0.85 for the gas phase calculation, while they on the other hand decrease the intercept. Therefore, the data sets with solvation and without solvation are almost equally spaced below and above the optimal correlations in red, respectively. The highest value of R^2 (0.9802) and best slope (1.02) are obtained by employing the SMD model, but the intercept is not as good as for IEFPCM and CPCM. Nevertheless, we will employ the IEFPCM implicit solvation model in all following calculations, because both the data points and the intercept are closer to the optimal correlation, and because the IEFPCM solvation model has been preferred in earlier relevant studies.[64,66,71,76,89]

Considering individual molecules in Fig. 8, we observe that the outliers from the linear regression lines are now different compounds than in the gas phase calculations. While DMeAzirA now perfectly lies on the correlation line, the calculated potentials of TEtPD and BPyrB are now too large and the one of DMeAzetA is too small.

Basis set analysis. In an earlier study,[71] it was reported that only a 10% improvement is obtained by changing the 6-31+G(d) basis set to the more 'expensive' 6-311++G(3df,2pd). However, today's computational power can easily handle the increased cost for the relative small compounds of the present study and therefore, a basis set analysis was performed for a subset of the present set of molecules in the hope of further improving the agreement with the optimal correlation. The basis set analysis was carried out for BMorphB, BPyrB, TMePD, DMeAzirA and DMePiprzA using the B3LYP functional and the IEFPCM solvation model. The results are visualized in Fig. 9. Within the Pople style basis sets we have investigated both adding more polarization functions, 6-31G(df,pd), and going to the triple zeta basis set augmented with diffuse functions, 6-311++G(d,p). The additional polarization functions have very little effect on the calculated potentials. But changing to a triple zeta basis set with diffuse functions (6-311++G(d,p)) significantly increases the calculated oxidation potentials and thereby moves the intercept much closer to the absolute potential of the Fc/Fc$^+$ redox couple. The larger oxidation potential is expected, because the increased number of compact valence functions describes the compressed radical cation better and thereby lower its energy to a larger extent than for the neutral compound. Furthermore, the data points of the selected five compounds exhibit now a perfect correlation with the experimental values.

Comparing the results of the Pople double and triple zeta basis sets with the results of their corresponding Dunning and Jensen basis sets, one observes that the potentials increase in the series Pople, Dunning and Jensen. Furthermore, all the basis sets without additional diffuse functions predict the potential of BPyrB to be too large. This is in particular the case for the cc-pVDZ and even more pc-1 basis sets but much less so for cc-pVTZ and least for pc-2 basis set. Secondly, both for the Pople and Dunning basis sets the potentials calculated with the triple zeta basis sets are closer to the ideal correlation line than the double zeta results. For the Jensen basis sets the opposite is the case both in the augmented and non-augmented version. Adding extra diffuse functions, improves for all three types of basis sets the correlation *i.e.* brings the BPyrB data point in line with the other ones. For the Dunning basis set, cc-pVDZ, adding the diffuse functions also further increases the potentials and brings them thus closer to the idea correlation line, while for the corresponding Jensen basis set, pc-1, the opposite

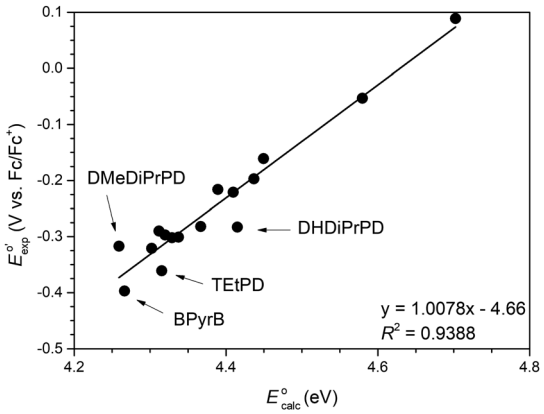

Fig. 10 Plot of the experimental $E^{\circ\prime}_{exp}$ *vs.* E°_{calc} calculated at the B3LYP/6-311++G(d,p)/IEFPCM level of theory.

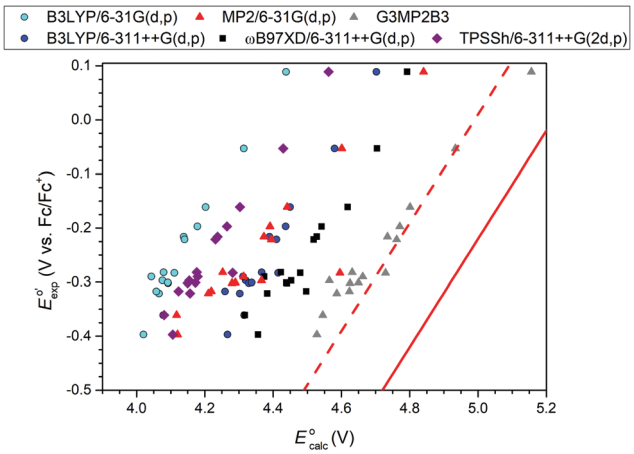

Fig. 11 Plot of the experimental $E^{\circ\prime}_{exp}$ *vs.* E°_{calc} calculated including the implicit solvation model IEFPCM and the methods: B3LYP/6-31G(d,p), MP2/6-31G(d,p), G3MP2B3, B3LYP/6-311++G(d,p), ωB97XD/6-311++G(d,p) and TPSSh/6-311++G(2d,p). The ideal correlation lines with intercept −5.22 V (---) and −4.99 V (- -) are shown.

happens. The results closest to the ideal line, on the other hand, are obtained with the aug-pc-0 basis set, an unpolarised but augmented double zeta basis set. However, the fact that the data point for DMeAzirA again is an outlier disqualifies this basis set. The basis set yielding the set of results next closest to the ideal line is 6-311++G(d,p). Combined with the fact that it also exhibits the best correlation, makes it in our eyes the best basis set among the ones investigated.

Overall, this analysis shows that the intercept is highly affected by the size of the basis set. Furthermore, the energies obtained from the larger basis sets augmented with diffuse functions are very similar, which means that the energies converge and the complete basis set limit of E°_{calc} for the B3LYP functional is approached.

The 6-311++G(d,p) basis set was thus chosen for calculating the potentials for the full series of compounds (Fig. 10), and the obtained least square fitting parameters are summarized in Table 3. By comparing to the original basis set, 6-31G(d,p), it becomes clear that although the slope is now perfect with 1.00 the overall quality of the correlation for the full set of molecules is reduced by 3% upon adding the additional valence and diffuse functions in the 6-311++G(d,p) basis set. Furthermore, also the intercept is slightly worse than with the smaller basis set. Therefore, we conclude that increasing the quality of the basis set is not alone sufficient to improve our computational strategy for calculating the oxidation potentials, and we therefore look towards an improvement of the quantum chemical methods.

Electron correlation analysis. In order to investigate whether a different choice of quantum chemical method could further improve the correlations, two other DFT functionals, ωB97XD and TPSSh, and two correlated wave function methods, MP2 and the combination method G3MP2B3, were selected. Table 3 and Fig. 11 summarise the results.

We notice that all methods predict higher oxidation potentials than the B3LYP/6-31G(d,p) level of theory (all data points move to the right). For ωB97XD/6-311++G(d,p) and TPSSh/6-311++G(2d,p) this must partly be due to the larger basis set, as seen for B3LYP in the previous section. Comparison with the B3LYP/6-311++G(d,p) results reveals a small decrease of ∼0.03 in the R^2-value for ωB97XD and also a smaller slope. On the other hand, the ωB97XD potentials are consistently closer to the optimal line. For TPSSh/6-311++G(2d,p) the R^2-value is marginally larger than for B3LYP/6-311++G(d,p) but the slope is still not as perfect as for B3LYP and the potentials are all smaller than both the B3LYP and ωB97XD values. On the other hand, the number of clear outliers from the correlation line is with two (BPyrB and DHDiPrPD) smaller than the four for both B3LYP (BPyrB, TEtPD, DHDiPrPD and DMeDiPrPD) and ωB97XD (DMeAzirA, DMeAzetA, DMeDiPrPD and TEtPD). The MP2 results, calculated with the smaller 6-31G(d,p) basis set without diffuse functions, are also significantly closer to the optimal lines than the corresponding B3LYP results. Actually, most of them are close to the oxidation potentials calculated with the B3LYP/6-311++G(d,p) method.

However, the slope is with 0.66 far away from the optimal value and even the B3LYP value obtained with the same basis set and the intercept, −3.12 V, is thus also far away from either of the ideal values. One should though recall that results obtained with the MP2 method are known to improve with the basis set size, and one might expect that the chosen basis set is not yet converged for this type of calculation.

The oxidation potentials calculated at the G3MP2B3 level of theory result in the highest value of R^2 (0.9624) and are located very close to the optimal red dashed line. The latter might be expected, because the Fc/Fc$^+$ oxidation potential of −4.99 V was calculated from the very similar computational method G3(MP2)-RAD-full-TZ.[157] Unfortunately, even though the data points are located close to the dashed line, the slope is only 0.74 resulting in an intercept of −3.72 V, and the method does not succeed in fulfilling all of the three criteria. The high value of R^2 for G3MP2B3 was expected, since the method has been parameterized for calculating thermodynamic properties as

for example oxidation potentials, and the total electronic energy is calculated at the computational expensive QCISD(T) level. The difference between the DFT/B3LYP and G3MP2B3 methods is in the calculation of the ΔE_{elec} term, which as mentioned earlier is by far the most important contribution to the Gibbs free energy.

In general, we conclude that correlation is an important factor to take into account, and the correlated wavefunction methods included in our study give results in closer agreement with the optimal line than DFT but the results are not as consistent as the ones obtained with the DFT functionals studied here. Among the three investigated DFT functionals there is a small preference for TPSSh/6-311++G(2d,p) due to the larger R^2 value and smaller number of outliers.

Dispersion effects. One of the differences between the B3LYP and ωB97XD functionals is that ωB97XD includes a dispersion correction in addition to ωB97XD being a range-separated functional meaning that the percentage of Hartree–Fock exchange included in the functional varies with the distance between electrons. In order to investigate whether the difference between the B3LYP and ωB97XD results is due to the inclusion of dispersion or not, we have carried out additional calculations with the B3LYP functional, where the Grimme D3(BJ) dispersion correction was added.[154]

The comparison of these B3LYP-GD3BJ results with the B3LYP and ωB97XD results, all with the 6-311++G(d,p) basis set is shown in Fig. 12 and Table 3. It becomes quite clear that the empirical dispersion correction cannot be the explanation for the differences between the B3LYP and ωB97XD results. Actually, adding the GD3(BJ) dispersion correction to the B3LYP functional has for most molecules only a small and not consistent effect. The improvement observed with the ωB97XD functional in Fig. 11 and 12 is thus a consequence of it being a range-separated functional with the amount of Hartree–Fock exchange varying between 22% at short range and 100% at long range.

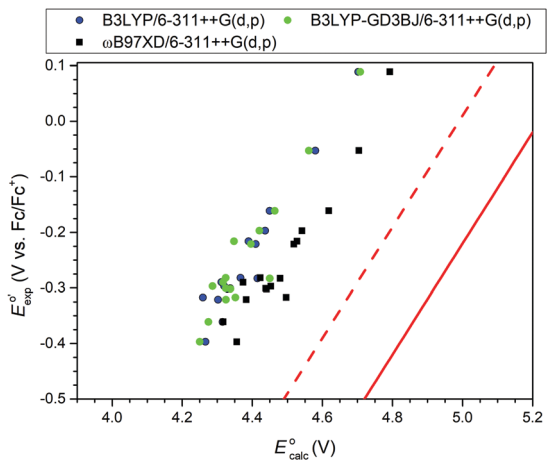

Fig. 12 Plot of the experimental $E^{\circ\prime}_{exp}$ *vs.* E°_{calc} calculated including the implicit solvation model IEFPCM and the methods: B3LYP/6-311++G(d,p), B3LYP-GD3BJ/6-311++G(d,p) and ωB97XD/6-311++G(d,p). The ideal correlation lines with intercept −5.22 V (---) and −4.99 V (- -) are shown.

Conclusions

We present a series of structurally closely related *N*,*N*,*N*′,*N*′ tetrasubstituted *p*-phenylenediamines, where the π-system suffers only small perturbations introduced by the N-substituents. The formal potentials for the reversible one-electron oxidation to the radical cations are obtained by CV and DPV. We investigate the performance of several computational models in reproducing the measured oxidation potentials. For this purpose, the experimental values are plotted against the calculated oxidation potentials and the correlation is evaluated based on the linear regression least square method. At the B3LYP/6-31G(d,p) level of theory the correlation between the experimentally determined potentials and the highest occupied molecular orbital, E_{HOMO}, in the neutral compound reveals a low correlation (R^2 = 0.8172 and slope 0.29). An improvement is observed when introducing electronic and geometric relaxation of the radical cation by calculating the adiabatic ionization potential, IP_a (R^2 = 0.8995 and slope 0.72). Including the thermal and entropic effects in the calculations of the oxidation potentials further improves the results to a slope of 0.85. The impact of including implicit solvation models (IEFPCM, CPCM, and SMD), larger basis sets, and correlation methods are also tested. The PCM implicit solvation models lead to major improvements of all three values of the regression *i.e.* the slope, the intercept and R^2 value. The slopes differ by less than 10% from the ideal value of 1.00 and the R^2 values are between 0.94 and 0.98.

The basis set analysis performed using the B3LYP functional for a selection of the compounds reveals that diffuse functions are important for improving the absolute values of the calculated oxidation potentials and their correlation with experiment. Finally, the oxidation potentials are calculated also with the B3LYP-GB3BJ, ωB97XD and TPSSh functionals, the MP2 method and the G3MP2B3 approach. The latter leads to the best (R^2 = 0.9624), but the slope and intercept are significantly worse than with the DFT functionals. The best slope is obtained with B3LYP/6-311++G(d,p) while TPSSh/6-311++G(2d,p) yields the most consistent results and only a slightly less perfect slope. In general we conclude that basis set size and treatment of electron correlation are important to take into account when calculating oxidation potentials for compounds with only small structural differences, where the electronic energy differences are the most important terms.

Author contributions

CLA carried out the CV and DPV measurements. CLA, EGL and OH did the computational work and JBC carried out the synthesis and characterization of the 15 compounds not commercially available: The project was supervised by OH and SPAS and all authors contributed to drafting the manuscript and the ESI.†

Conflicts of interest

There are no conflicts to declare.

Acknowledgements

E. G. L. thanks CNPq and the Science without Borders program for a postdoc fellowship, 206886/2014-4. S. P. A. S. thanks the Danish Agency for Science, Technology and Innovation for an International Network Programme grant 1370-00075B.

Notes and references

1 A. J. Bard, M. Stratmann and H. Schäfer, *Encyclopedia of electrochemistry*, Wiley-VCH, Weinheim, 2004.
2 O. Hammerich and B. Speiser, *Organic Electrochemistry: Revised and Expanded*, 5th edn, CRC Press, Boca Raton, 2015.
3 D. Astruc, *New J. Chem.*, 2009, **33**, 1191–1206.
4 E. Steckhan, *Top. Curr. Chem.*, 1987, **142**, 1–69.
5 M. Majek and A. Jacobi von Wangelin, *Acc. Chem. Res.*, 2016, **49**, 2316–2327.
6 S. Hammes-Schiffer, *Acc. Chem. Res.*, 2018, **51**, 1975–1983.
7 H.-J. Himmel, *Synlett*, 2018, 1957–1977.
8 S. R. Forrest and M. E. Thompson, *Chem. Rev.*, 2007, **107**, 923–925.
9 R. J. Mortimer, *Chem. Soc. Rev.*, 1997, **26**, 147–156.
10 S. Günes, H. Neugebauer and N. S. Sariciftci, *Chem. Rev.*, 2007, **107**, 1324–1338.
11 J. L. Segura, N. Martin and D. M. Guldi, *Chem. Soc. Rev.*, 2005, **34**, 31–47.
12 P. Batail, *Chem. Rev.*, 2004, **104**, 4887–5782.
13 J. Heinze, B. A. Frontana-Uribe and S. Ludwigs, *Chem. Rev.*, 2010, **110**, 4724–4771.
14 H. B. Gray and J. R. Winkler, *Chem. Phys. Lett.*, 2009, **483**, 1–9.
15 S. Prabhulkar, H. Tian, X. Wang, J.-J. Zhu and C.-Z. Li, *Antioxid. Redox Signal.*, 2012, **17**, 1796–1822.
16 P. Hosseinzadeh and Y. Lu, *Biochim. Biophys. Acta, Bioenerg.*, 2016, **1857**, 557–581.
17 R. Razeghifard, *Photosynth. Res.*, 2008, **98**, 677–685.
18 W. Song, Z. Chen, M. K. Brennaman, J. J. Concepcion, A. O. T. Patrocinio, N. Y. M. Iha and T. J. Meyer, *Pure Appl. Chem.*, 2011, **83**, 749–768.
19 S. J. Mora, E. Odella, G. F. Moore, D. Gust, T. A. Moore and A. L. Moore, *Acc. Chem. Res.*, 2018, **51**, 445–453.
20 N. T. La Porte, J. F. Martinez, S. Chaudhuri, S. Hedstrom, V. S. Batista and M. R. Wasielewski, *Coord. Chem. Rev.*, 2018, **361**, 98–119.
21 G. J. Kavarnos and N. J. Turro, *Chem. Rev.*, 1986, **86**, 401–449.
22 L. Eberson, *Adv. Phys. Org. Chem.*, 1982, **18**, 79–185.
23 R. A. Marcus and N. Sutin, *Biochim. Biophys. Acta, Rev. Bioenerg.*, 1985, **811**, 265–322.
24 L. E. Eberson, *Electron transfer reactions in organic chemistry*, Springer, Berlin, 1987.
25 M. A. Fox, *Photochem. Photobiol.*, 1990, **52**, 617–627.
26 I. R. Gould and S. Farid, *Acc. Chem. Res.*, 1996, **29**, 522–528.
27 *Electron transfer in chemistry*, ed. D. Astruc, V. Balzani, A. P. De Silva, S. Fukuzumi, I. R. Gould, H. B. Gray, Y. Haas, T. E. Mallouk, J. Mattay, P. Piotrowiak and M. A. J. Rodgers, Wiley-VCH, Weinheim, 2001.
28 A. J. Bard and L. R. Faulkner, *Electrochemical methods: fundamentals and applications*, 2nd edn, Wiley, New York, 2001.
29 O. Hammerich and V. D. Parker, *Adv. Phys. Org. Chem.*, 1984, **20**, 55–189.
30 K. Yoshida, *Electrooxidation in organic chemistry: the role of cation radicals as synthetic intermediates*, Wiley, New York, 1984.
31 O. Hammerich and M. F. Nielsen, *Acta Chem. Scand.*, 1998, **52**, 831–857.
32 S. Torii, *Electroorganic Reduction Synthesis*, Wiley-VCH, Weinheim, 2006.
33 K. D. Moeller, *Chem. Rev.*, 2018, **118**, 4817–4833.
34 K. J. Tupper, J. J. Gajewski and R. W. Counts, *THEOCHEM*, 1991, **81**, 263–275.
35 H.-J. Wang and C.-J. Yu, *Res. Chem. Intermed.*, 2010, **36**, 1003–1019.
36 P. P. Romanczyk, G. Rotko and S. S. Kurek, *Electrochem. Commun.*, 2014, **48**, 21–23.
37 H. M. Muchall, N. H. Werstiuk and B. Choudhury, *Can. J. Chem.*, 1998, **76**, 221–227.
38 I. A. Topol, C. McGrath, E. Chertova, C. Dasenbrock, W. R. Lacourse, M. A. Eissenstat, S. K. Burt, L. E. Henderson and J. R. Casas-Finet, *Protein Sci.*, 2001, **10**, 1434–1445.
39 P. Winget, C. J. Cramer and D. G. Truhlar, *Theor. Chem. Acc.*, 2004, **112**, 217–227.
40 A. Maccoll, *Nature*, 1949, **163**, 178–179.
41 L. E. Lyons, *Nature*, 1950, **166**, 193.
42 A. Pullman, B. Pullman and G. Berthier, *Bull. Soc. Chim. Fr.*, 1950, 591–594.
43 G. J. Hoijtink and J. van Schooten, *Rec. Trav. Chim. Pays-Bas Belg.*, 1953, **72**, 691–705.
44 G. J. Hoijtink, *Rec. Trav. Chim. Pays-Bas Belg.*, 1955, **74**, 1525–1539.
45 G. J. Hoijtink, *Rec. Trav. Chim. Pays-Bas Belg.*, 1958, **77**, 555–558.
46 M. E. Peover, *Nature*, 1962, **193**, 475–476.
47 E. S. Pysh and N. C. Yang, *J. Am. Chem. Soc.*, 1963, **85**, 2124–2130.
48 W. C. Neikam and M. M. Desmond, *J. Am. Chem. Soc.*, 1964, **86**, 4811–4814.
49 C. Parkanyi and R. Zahradník, *Coll. Czech. Chem. Commun.*, 1965, **30**, 4287–4296.
50 R. Zahradnik and C. Parkanyi, *Talanta*, 1965, **12**, 1289–1297.
51 J. Koutecky, *Z. Phys. Chem.*, 1967, **52**, 8–26.
52 G. J. Gleicher and M. K. Gleicher, *J. Phys. Chem.*, 1967, **71**, 3693–3696.
53 O. G. Mekenyan, S. P. Bradbury and V. B. Kamenska, *SAR QSAR Environ. Res.*, 1996, **5**, 255–268.
54 G. A. DiLabio, D. A. Pratt and J. S. Wright, *Chem. Phys. Lett.*, 1999, **311**, 215–220.
55 M. Namazian, H. A. Almodarresieh, M. R. Noorbala and H. R. Zare, *Chem. Phys. Lett.*, 2004, **396**, 424–428.
56 M. Namazian and P. Norouzi, *J. Electroanal. Chem.*, 2004, **573**, 49–53.
57 L. D. Hicks, A. J. Fry and V. C. Kurzweil, *Electrochim. Acta*, 2004, **50**, 1039–1047.

58 R. Benassi, P. Ferrarini, C. Fontanesi, L. Benedetti and F. Paolucci, *J. Electroanal. Chem.*, 2004, **564**, 231–237.
59 A. Modelli, L. Mussoni and D. Fabbri, *J. Phys. Chem. A*, 2006, **110**, 6482–6486.
60 K. Alizadeh, S. Seyyedi and M. Shamsipur, *Pol. J. Chem.*, 2008, **82**, 1449–1456.
61 K. Alizadeh and M. Shamsipur, *THEOCHEM*, 2008, **862**, 39–43.
62 X. Wu, A. P. Davis, P. C. Lambert, L. Kraig Steffen, O. Toy and A. J. Fry, *Tetrahedron*, 2009, **65**, 2408–2414.
63 A. Kuhn, K. G. Eschwege and J. Conradie, *J. Phys. Org. Chem.*, 2012, **25**, 58–68.
64 J. H. Chen, L. M. He and R. L. Wang, *J. Phys. Chem. A*, 2013, **117**, 5132–5139.
65 R. S. Assary, F. R. Brushett and L. A. Curtiss, *RSC Adv.*, 2014, **4**, 57442–57451.
66 A. P. Davis and A. J. Fry, *J. Phys. Chem. A*, 2010, **114**, 12299–12304.
67 K. S. Raymond, A. K. Grafton and R. A. Wheeler, *J. Phys. Chem. B*, 1997, **101**, 623–631.
68 M. Shamsipur, A. Siroueinejad, B. Hemmateenejad, A. Abbaspour, H. Sharghi, K. Alizadeh and S. Arshadi, *J. Electroanal. Chem.*, 2007, **600**, 345–358.
69 M. T. Huynh, C. W. Anson, A. C. Cavell, S. S. Stahl and S. Hammes-Schiffer, *J. Am. Chem. Soc.*, 2016, **138**, 15903–15910.
70 M.-H. Baik and R. A. Friesner, *J. Phys. Chem. A*, 2002, **106**, 7407–7412.
71 Y. Fu, L. Liu, H.-Z. Yu, Y.-M. Wang and Q.-X. Guo, *J. Am. Chem. Soc.*, 2005, **127**, 7227–7234.
72 J. Moens, P. Jaque, F. De Proft and P. Geerlings, *J. Phys. Chem. A*, 2008, **112**, 6023–6031.
73 H. G. Roth, N. A. Romero and D. A. Nicewicz, *Synlett*, 2016, 714–723.
74 J. L. Borioni, M. Puiatti, A. B. Pierini and D. M. A. Vera, *Phys. Chem. Chem. Phys.*, 2017, **19**, 9189–9198.
75 H. Neugebauer, F. Bohle, M. Bursch, A. Hansen and S. Grimme, *J. Phys. Chem. A*, 2020, **124**, 7166–7176.
76 P. Winget, E. J. Weber, C. J. Cramer and D. G. Truhlar, *Phys. Chem. Chem. Phys.*, 2000, **2**, 1231–1239.
77 R. I. Zubatyuk, L. Gorb, O. V. Shishkin, M. Qasim and J. Leszczynski, *J. Comput. Chem.*, 2010, **31**, 144–150.
78 C. K. Chua, M. Pumera and L. Rulisek, *J. Phys. Chem. C*, 2012, **116**, 4243–4251.
79 N. Ree, C. L. Andersen, M. D. Kilde, O. Hammerich, M. B. Nielsen and K. V. Mikkelsen, *Phys. Chem. Chem. Phys.*, 2018, **20**, 7438–7446.
80 M. Namazian, P. Norouzi and R. Ranjbar, *THEOCHEM*, 2003, **625**, 235–241.
81 J. Tomasi, B. Mennucci and R. Cammi, *Chem. Rev.*, 2005, **105**, 2999–3093.
82 S. Miertuš, E. Scrocco and J. Tomasi, *Chem. Phys.*, 1981, **55**, 117–129.
83 E. Cancès, B. Mennucci and J. Tomasi, *J. Chem. Phys.*, 1997, **107**, 3032–3041.
84 E. Cancès and B. Mennucci, *J. Math. Chem.*, 1998, **23**, 309–326.
85 V. Barone and M. Cossi, *J. Phys. Chem. A*, 1998, **102**, 1995–2001.
86 M. Cossi, N. Rega, G. Scalmani and V. Barone, *J. Comput. Chem.*, 2003, **24**, 669–681.
87 A. V. Marenich, C. J. Cramer and D. G. Truhlar, *J. Phys. Chem. B*, 2009, **113**, 6378–6396.
88 J. D. Thompson, C. J. Cramer and D. G. Truhlar, *J. Phys. Chem. A*, 2004, **108**, 6532–6542.
89 A. V. Marenich, J. Ho, M. L. Coote, C. J. Cramer and D. G. Truhlar, *Phys. Chem. Chem. Phys.*, 2014, **16**, 15068–15106.
90 J. Ho, M. Coote, C. Cramer and D. Truhlar, in *Organic Electrochemistry*, ed. O. Hammerich and B. Speiser, CRC Press, Boca Raton, 5th edn, 2015, ch. 6, pp. 229–259.
91 J. O. Howell, J. M. Goncalves, C. Amatore, L. Klasinc, R. M. Wightman and J. K. Kochi, *J. Am. Chem. Soc.*, 1984, **106**, 3968–3976.
92 T. Buch-Rasmussen, B. R. Olsen, J. Kulys, K. Bechgaard, J. B. Christensen, J. Wang, M. S. Ozsoz, F. Colin and O. Garcia, WO9207263A1, 1992.
93 J. Kulys, T. Buch-Rasmussen, K. Bechgaard, V. Razumas, J. Kazlauskaite, J. Marcinkeviciene, J. B. Christensen and H. E. Hansen, *J. Mol. Catal.*, 1994, **91**, 407–420.
94 J. B. Christensen, N.-C. Schioedt, K. Bechgaard and T. Buch-Rasmussen, *Acta Chem. Scand.*, 1996, **50**, 1013–1019.
95 O. Hammerich, T. Hansen, A. Thorvildsen and J. B. Christensen, *ChemPhysChem*, 2009, **10**, 1805–1824.
96 M. Zalibera, P. Rapta, G. Gescheidt, J. B. Christensen, O. Hammerich and L. Dunsch, *J. Phys. Chem. C*, 2011, **115**, 3942–3948.
97 T. Yao, S. Musha and M. Munemori, *Chem. Lett.*, 1974, 939–944.
98 G. Grampp and P. Pluschke, *Coll. Czech. Chem. Commun.*, 1987, **52**, 819–829.
99 A. J. Pearson, A. M. Gelormini, M. A. Fox and D. Watkins, *J. Org. Chem.*, 1996, **61**, 1297–1305.
100 A. J. Pearson and A. M. Gelormini, *Tetrahedron Lett.*, 1997, **38**, 5123–5126.
101 G. Schwarzenbacher, B. Evers, I. Schneider, A. de Raadt, J. Besenhard and R. Saf, *J. Mater. Chem.*, 2002, **12**, 534–539.
102 E. Deunf, F. Dolhem, D. Guyomard, J. Simonet and P. Poizot, *Electrochim. Acta*, 2018, **262**, 276–281.
103 C. Wurster and E. Schobig, *Ber. Dtsch. Chem. Ges.*, 1879, **12**, 1807–1813.
104 S. F. Nelsen, M. N. Weaver, J. P. Telo, B. L. Lucht and S. Barlow, *J. Org. Chem.*, 2005, **70**, 9326–9333.
105 A. M. Brouwer and R. Wilbrandt, *J. Phys. Chem.*, 1996, **100**, 9678–9688.
106 A. M. Brouwer, *J. Phys. Chem. A*, 1997, **101**, 3626–3633.
107 G. Grampp and W. Jaenicke, *Ber. Bunsen-Ges. Phys. Chem.*, 1984, **88**, 325–334.
108 G. Grampp and W. Jaenicke, *Ber. Bunsen-Ges. Phys. Chem.*, 1984, **88**, 335–340.
109 K. Elbl-Weiser, F. A. Neugebauer and H. A. Staab, *Tetrahedron Lett.*, 1989, **30**, 6161–6164.
110 F. A. Neugebauer, B. Funk and H. A. Staab, *Tetrahedron Lett.*, 1994, **35**, 4755–4758.

111 G. Grampp, A.-M. Kelterer, S. Landgraf, M. Sacher, D. Niethammer, J. P. Telo, R. M. B. Dias and A. J. S. C. Vieira, *Monatsh. Chem.*, 2005, **136**, 519–536.
112 A. Rogowska, S. Kuhl, R. Schneider, A. Walcarius and B. Champagne, *Phys. Chem. Chem. Phys.*, 2007, **9**, 828–836.
113 K. Hu and D. H. Evans, *J. Electroanal. Chem.*, 1997, **423**, 29–35.
114 N. E. Gruhn, N. A. Macias-Ruvalcaba and D. H. Evans, *J. Phys. Chem. A*, 2006, **110**, 5650–5655.
115 V. Coropceanu, N. E. Gruhn, S. Barlow, C. Lambert, J. C. Durivage, T. G. Bill, G. Noell, S. R. Marder and J.-L. Bredas, *J. Am. Chem. Soc.*, 2004, **126**, 2727–2731.
116 D. Dehareng, G. Dive and A. Moradpour, *Int. J. Quantum Chem.*, 2000, **76**, 552–573.
117 S. F. Nelsen, H. Q. Tran and M. A. Nagy, *J. Am. Chem. Soc.*, 1998, **120**, 298–304.
118 K. Y. Chiu, T.-H. Su, C. W. Huang, G.-S. Liou and S.-H. Cheng, *J. Electroanal. Chem.*, 2005, **578**, 283–287.
119 M. Goez, *Z. Phys. Chem.*, 1990, **169**, 123–132.
120 M. Goez, *Z. Phys. Chem.*, 1990, **169**, 133–145.
121 G. Rauhut and T. Clark, *J. Am. Chem. Soc.*, 1993, **115**, 9127–9135.
122 S. V. Rosokha and J. K. Kochi, *J. Am. Chem. Soc.*, 2007, **129**, 3683–3697.
123 S. F. Nelsen and M. J. R. Yunta, *J. Phys. Org. Chem.*, 1994, **7**, 55–62.
124 K. Kimura, H. Yamada and H. Tsubomura, *J. Chem. Phys.*, 1968, **48**, 440–444.
125 K. Yokoyama and S. Maeda, *Chem. Phys. Lett.*, 1977, **48**, 59–62.
126 G. Grampp, S. Landgraf, K. Rasmussen and S. Strauss, *Spectrochim. Acta, Part A*, 2002, **58**, 1219–1226.
127 U. Nickel and W. Jaenicke, *Ber. Bunsenges. Phys. Chem.*, 1982, **86**, 695–701.
128 G. Zhu, Q. Li, X. Guo and Z. Liu, *J. Mol. Liq.*, 2020, **312**, 113394.
129 D. Sun, S. V. Rosokha and J. K. Kochi, *J. Phys. Chem. B*, 2007, **111**, 6655–6666.
130 M. A. Lopatin, M. P. Shurygina, T. I. Lopatina and A. S. Kazarin, *Russ. J. Gen. Chem.*, 2013, **83**, 2320–2323.
131 S. V. Rosokha and E. A. Loboda, *J. Phys. Chem. A*, 2015, **119**, 3833–3842.
132 S. Kuss and R. G. Compton, *Electrochim. Acta*, 2017, **242**, 19–24.
133 R. A. S. Couto, L. Chen, S. Kuss and R. G. Compton, *Analyst*, 2018, **143**, 4840–4843.
134 A. Petrova, M. Mamedov, B. Ivanov, A. Semenov and M. Kozuleva, *Photosynth. Res.*, 2018, **137**, 421–429.
135 W. R. Fawcett and C. A. Foss, Jr., *J. Electroanal. Chem. Interfacial Electrochem.*, 1989, **270**, 103–118.
136 H. Svith, H. Jensen, J. Almstedt, P. Andersson, T. Lundbäck, K. Daasbjerg and M. Jonsson, *J. Phys. Chem. A*, 2004, **108**, 4805–4811.
137 G. Gritzner and J. Kuta, *Pure Appl. Chem.*, 1984, **56**, 461–466.
138 J. E. Bartmess, *J. Phys. Chem.*, 1994, **98**, 6420–6424.
139 A. D. Becke, *J. Chem. Phys.*, 1993, **98**, 5648–5652.
140 R. Ditchfield, W. J. Hehre and J. A. Pople, *J. Chem. Phys.*, 1971, **54**, 724–728.
141 W. J. Hehre, R. Ditchfield and J. A. Pople, *J. Chem. Phys.*, 1972, **56**, 2257–2261.
142 T. Clark, J. Chandrasekhar, G. W. Spitznagel and P. v. R. Schleyer, *J. Comput. Chem.*, 1983, **4**, 294–301.
143 M. J. Frisch, J. A. Pople and J. S. Binkley, *J. Chem. Phys.*, 1984, **80**, 3265–3269.
144 J. T. H. Dunning, *J. Chem. Phys.*, 1989, **90**, 1007–1023.
145 R. A. Kendall, T. H. Dunning and R. J. Harrison, *J. Chem. Phys.*, 1992, **96**, 6796–6806.
146 F. Jensen, *J. Chem. Phys.*, 2001, **115**, 9113–9125.
147 F. Jensen, *J. Chem. Phys.*, 2002, **116**, 7372–7379.
148 J. D. Chai and M. Head-Gordon, *Phys. Chem. Chem. Phys.*, 2008, **10**, 6615–6620.
149 J. Tao, J. P. Perdew, V. N. Staroverov and G. E. Scuseria, *Phys. Rev. Lett.*, 2003, **91**, 146401.
150 V. N. Staroverov, G. E. Scuseria, J. Tao and J. P. Perdew, *J. Chem. Phys.*, 2003, **119**, 12129–12137.
151 C. Møller and M. S. Plesset, *Phys. Rev.*, 1934, **46**, 618–622.
152 J. A. Pople, J. S. Binkley and R. Seeger, *Int. J. Quantum Chem. Symp.*, 1976, **10**, 1–19.
153 A. G. Baboul, L. A. Curtiss, P. C. Redfern and K. Raghavachari, *J. Chem. Phys.*, 1999, **110**, 7650–7657.
154 S. Grimme, S. Ehrlich and L. Goerigk, *J. Comput. Chem.*, 2011, **32**, 1456–1465.
155 M. J. Frisch, G. W. Trucks, H. B. Schlegel, G. E. Scuseria, M. A. Robb, J. R. Cheeseman, G. Scalmani, V. Barone, B. Mennucci, G. A. Petersson, H. Nakatsuji, M. Caricato, X. Li, H. P. Hratchian, A. F. Izmaylov, J. Bloino, G. Zheng, J. L. Sonnenberg, M. Hada, M. Ehara, K. Toyota, R. Fukuda, J. Hasegawa, M. Ishida, T. Nakajima, Y. Honda, O. Kitao, H. Nakai, T. Vreven, J. J. A. Montgomery, J. E. Peralta, F. Ogliaro, M. Bearpark, J. J. Heyd, E. Brothers, K. N. Kudin, V. N. Staroverov, R. Kobayashi, J. Normand, K. Raghavachari, A. Rendell, J. C. Burant, S. S. Iyengar, J. Tomasi, M. Cossi, N. Rega, J. M. Millam, M. Klene, J. E. Knox, J. B. Cross, V. Bakken, C. Adamo, J. Jaramillo, R. Gomperts, R. E. Stratmann, O. Yazyev, A. J. Austin, R. Cammi, C. Pomelli, J. W. Ochterski, R. L. Martin, K. Morokuma, V. G. Zakrzewski, G. A. Voth, P. Salvador, J. J. Dannenberg, S. Dapprich, A. D. Daniels, Ö. Farkas, J. B. Foresman, J. V. Ortiz, J. Cioslowski and D. J. Fox, *Rev. B01*, Gaussian, Inc., Wallingford CT, 2010.
156 L. E. Roy, E. Jakubikova, M. G. Guthrie and E. R. Batista, *J. Phys. Chem. A*, 2009, **113**, 6745–6750.
157 M. Namazian, C. Y. Lin and M. L. Coote, *J. Chem. Theory Comput.*, 2010, **6**, 2721–2725.
158 C. Reichardt, *Solvents and Solvent Effects in Organic Chemistry*, 2nd edn, VCH, 1988.
159 P. Wang and A. Anderko, *Fluid Phase Equilib.*, 2001, **186**, 103–122.
160 E. G. Lacerda, Jr., F. S. Kamounah, K. Coutinho, S. P. A. Sauer, P. E. Hansen and O. Hammerich, *ChemPhysChem*, 2019, **20**, 78–91.
161 S. L. V. Zahn, O. Hammerich, S. P. A. Sauer and P. E. Hansen, *J. Comput. Chem.*, 2021, **42**, 1248–1262.